

Resonances in coated long period fiber gratings and cladding removed multimode optical fibers: a comparative study

Ignacio Del Villar,* Carlos R. Zamarreño, Miguel Hernaez, Francisco J. Arregui, and Ignacio R. Matias

Departamento de Ingeniería Eléctrica y Electrónica, Universidad Pública de Navarra, 31006 Pamplona, Spain
*ignacio.delvillar@unavarra.es

Abstract: Two optical fiber devices have been coated in parallel: a long period fiber grating (LPFG) and a cladding-removed multimode optical fiber (CRMOF). The progressive coating of the LPFG by means of the layer-by-layer electrostatic-self-assembly, permits to observe a resonance wavelength shift of the attenuation bands in the transmission spectrum. The cause of this wavelength shift is the reorganization of the cladding mode effective indices. The cause of this modal reorganization can be understood with the results observed in the CRMOF coated in parallel. A lossy-mode-resonance (LMR) is generated in the same wavelength range of the LPFG attenuation bands analyzed. Moreover, the thickness range where the wavelength shift of the LPFG attenuation bands occurs coincides exactly with the thickness range where the LMR can be visualized in the transmission spectrum. These phenomena are analyzed theoretically and corroborated experimentally. The advantages and disadvantages of both optical fiber devices are explained.

©2010 Optical Society of America

OCIS codes: (060.3735) Fiber optics and optical communications, Fiber Bragg gratings; (310.6805) Thin films, theory and design; (310.1860) Thin films, deposition and fabrication.

References and links

1. S. W. James, and R. P. Tatam, "Optical fibre long-period grating sensors: characteristics and application," *Meas. Sci. Technol.* **14**(5), R49–R61 (2003).
2. I. Del Villar, I. R. Matias, and F. J. Arregui, *Handbook of interferometers: research, technology and applications*, (New York, 2009).
3. N. D. Rees, S. W. James, R. P. Tatam, and G. J. Ashwell, "Optical fiber long-period gratings with Langmuir-Blodgett thin-film overlays," *Opt. Lett.* **27**(9), 686–688 (2002).
4. I. Del Villar, I. R. Matias, F. J. Arregui, and P. Lalanne, "Optimization of sensitivity in Long Period Fiber Gratings with overlay deposition," *Opt. Express* **13**(1), 56–69 (2005).
5. I. Del Villar, I. R. Matias, F. J. Arregui, and M. Achaerandio, "Nanodeposition of materials with complex refractive index in long-period fiber gratings," *J. Lightwave Technol.* **23**(12), 4192–4199 (2005).
6. Z. Y. Wang, J. R. Hefflin, R. H. Stolen, and S. Ramachandran, "Analysis of optical response of long period fiber gratings to nm-thick thin-film coating," *Opt. Express* **13**(8), 2808–2813 (2005).
7. I. Del Villar, I. R. Matias, and F. J. Arregui, "Influence on cladding mode distribution of overlay deposition on long-period fiber gratings," *J. Opt. Soc. Am. A* **23**(3), 651–658 (2006).
8. A. Cusano, A. Iadicicco, P. Pilla, L. Contessa, S. Campopiano, A. Cutolo, and M. Giordano, "Mode transition in high refractive index coated long period gratings," *Opt. Express* **14**(1), 19–34 (2006).
9. J. M. Corres, I. del Villar, I. R. Matias, and F. J. Arregui, "Fiber-optic pH-sensors in long-period fiber gratings using electrostatic self-assembly," *Opt. Lett.* **32**(1), 29–31 (2007).
10. P. Pilla, A. Iadicicco, L. Contessa, S. Campopiano, A. Cutolo, M. Giordano, G. Guerra, and A. Cusano, "Optical chemo-sensor based on long-period gratings coated with δ form syndiotactic polystyrene," *IEEE Photon. Technol. Lett.* **17**(8), 1713–1715 (2005).
11. D. W. Kim, Y. Zhang, K. L. Cooper, and A. Wang, "Fibre-optic interferometric immuno-sensor using long period grating," *Electron. Lett.* **42**(6), 324–325 (2006).
12. P. Pilla, P. Foglia Manzillo, M. Giordano, M. L. Korwin-Pawłowski, W. J. Bock, and A. Cusano, "Spectral behavior of thin film coated cascaded tapered long period gratings in multiple configurations," *Opt. Express* **16**(13), 9765–9780 (2008).
13. R. P. Murphy, S. W. James, and R. P. Tatam, "Multiplexing of Fiber-Optic Long-Period Grating-Based Interferometric Sensor," *J. Lightwave Technol.* **25**(3), 825–829 (2007).

14. I. Del Villar, C. M. Zamarreño, M. Hernaez, F. J. Arregui, and I. R. Matias, "Lossy mode resonance generation with Indium Tin Oxide coated optical fibers for sensing application," *J. Lightwave Technol.* **28**(1), 111–117 (2010).
15. M. Marciniak, J. Grzegorzewski, and M. Szustakowski, "Analysis of lossy mode cut-off conditions in planar waveguides with semiconductor guiding layer," *IEE Proceedings J.* **140**, 247–251 (1993).
16. D. Razansky, P. D. Einziger, and D. R. Adam, "Broadband absorption spectroscopy via excitation of lossy resonance modes in thin films," *Phys. Rev. Lett.* **95**(1), 018101 (2005).
17. F. Yang, and J. R. Sambles, "Determination of the optical permittivity and thickness of absorbing films using long range modes," *J. Mod. Opt.* **44**, 1155–1163 (1997).
18. T. E. Batchman, and G. M. McWright, "Mode coupling between dielectric and semiconductor planar waveguides," *IEEE J. Quantum Electron.* **18**(4), 782–788 (1982).
19. G. Decher, "Fuzzy nanoassemblies: Toward layered polymeric multicomposites," *Science* **277**(5330), 1232–1237 (1997).
20. J. Goicoechea, C. R. Zamarreño, I. R. Matias, and F. J. Arregui, "Optical fiber pH sensors based on layer-by-layer electrostatic self-assembled Neutral Red," *Sens. Actuators B Chem.* **132**(1), 305–311 (2008).
21. A. K. Sharma, and B. D. Gupta, "On the sensitivity and signal to noise ratio of a step-index fiber optic surface plasmon resonance sensor with bimetallic layers," *Opt. Commun.* **245**(1-6), 159–169 (2005).
22. Y. Xu, N. B. Jones, J. Fothergill, and C. Hanning, "Analytical estimates of the characteristics of surface Plasmon resonance fibre-optic sensors," *J. Mod. Opt.* **47**(6), 1099–1110 (2000).
23. R. C. Jorgenson, and S. S. Yee, "A fiber-optic chemical sensor based on surface Plasmon resonance," *Sens. Actuators B Chem.* **12**(3), 213–220 (1993).
24. G. P. Agrawal, *Nonlinear fiber optics*, p. 8., (3rd ed., Academic Press: New York, 2001).
25. Y. Yang, X. W. Sun, B. J. Chen, C. X. Xu, T. P. Chen, C. Q. Sun, B. K. Tay, and Z. Sun, "Refractive indices of textured indium tin oxide and zinc oxide thin films," *Thin Solid Films* **510**(1-2), 95–101 (2006).

1. Introduction

Long-period fiber gratings (LPFGs) consist of an index modulation of the core refractive index of a single mode fiber (SMF) with a much longer period than a conventional fiber Bragg grating (FBG). This permits to induce attenuation bands in the transmission spectrum based on the coupling between the core mode and the co-propagating cladding modes, differently from fiber Bragg gratings (FBGs), where coupling between contra-propagating core modes occurs. As a result LPFGs are strongly influenced by the surrounding medium due to cladding modes coupling. This interesting property has permitted LPFGs to find applicability both in optical communications and in optical sensing [1,2].

The first published work about LPFG nanometer-scale coating [3], has resulted in an increasing number of publications during the last years. The physical phenomena involved have been analyzed [4–8], and many interesting applications have been found such as pH sensors, chemical sensors and immunosensors [9–11]. The experimental setups have also evolved to more complex designs such as tapered LPFG coating [12] or even multiple parameter interrogation [13]. However, no matter the complexity of the experimental setup, an optimum in sensitivity is aimed for all sensors fabricated, which occurs when the effective index of cladding modes experiments a highest variation as a function of one of the following parameters: coating refractive index, coating thickness and surrounding medium refractive index [4]. A first approach permitted to explain that the cladding mode reorganization is induced by the transition of a cladding mode that is guided now in the coating [4,8]. However, a thorough analysis of the phenomenon permits to observe that the reorganization is caused by two modes guided in the coating [7]. The consequence of this cladding mode reorganization is an abrupt wavelength shift of LPFG resonances, which are dependent on the cladding mode propagation constants and satisfy the following condition:

$$\beta_{01}(\lambda) + s_0 \zeta_{01,01}(\lambda) - (\beta_{0j}(\lambda) + s_0 \zeta_{0j,0j}(\lambda)) = \frac{2\pi N}{\Lambda} \quad (1)$$

where ζ_{0l} and ζ_{0j} are the propagation constants of the core and the j cladding modes respectively, $\zeta_{01,01}$ and $\zeta_{0j,0j}$ are the self-coupling coefficients of the core and the j cladding modes, s_0 is the coefficient of the first Fourier component of the grating, Λ is the period of the grating, and N is the diffraction order.

Unfortunately, only the consequence of modes being guided in the coating, which is the wavelength shift of the LPFG resonances, could be observed in the experiments. Recently, it

has been proved the fabrication of sensors based on coating a cladding-removed multimode optical fiber (CRMOF) [14]. One or more resonances can be generated in the transmission spectrum depending of the coating properties [14–18]. Each of these resonances is generated by coupling of the evanescent field guided by the fiber to lossy modes guided in the coating. Hence, these resonances will be considered as lossy mode resonances (LMR).

In this work, a coating is deposited on both devices (LPFG and CRMOF) in parallel to see that the resonances generated in each one are closely related. The sensitivity of both devices is compared and the main issues of both devices are discussed

2. Experimental section

In this section, the fabrication and characterization of the devices used in this work is presented.

2.1 Device fabrication

As it was mentioned in the introduction two devices are used in the experiments. The LPFG was purchased from O/E Land. It was written in an HI1060 Corning single-mode fiber (core diameter 5 μm , cladding diameter 125 μm) and the grating period is 200 μm . For the CRMOF the following procedure is used. First, a 2.5 cm fragment of FT200EMT optical fiber from Thorlabs Inc. (core diameter 200 μm , cladding diameter 225 μm , full acceptance cone 46°) was prepared. The 25 μm plastic cladding of the fiber was chemically removed by sonication in piranha, detergent, ultrapure water and acetone solutions successively. Afterwards, it was perpendicularly cleaved and spliced to 200 μm optical fiber core pigtails at both extremes to monitorize the transmission spectra of the device during the fabrication.

Both devices were coated in parallel by means of the Layer by Layer (LbL) method [19]. A polyacrylic acid (PAA) solution was used as anionic polyelectrolyte and a polyallylamine hydrochloride and neutral red (PAH/NR) solution as cationic polyelectrolyte [20]. The number of bilayers was 90. After each monolayer deposition, the devices were cleaned with ultrapure water. Then, they stayed in water for 10 seconds and in air for 30 seconds.

2.2 Device characterization

The transmission spectra were collected after each bilayer when the devices were immersed in water (after the cleaning procedure), using the experimental setup shown in Fig. 1. For the CRMOF it consists of a white light source (Ando AQ-4303B) connected to one of the optical fiber pigtails. The other one is connected to a NIR512 spectrometer from Oceanoptics Inc. This allows covering a range of wavelengths from 1250 to 1650 nm. For the LPFG the setup consists of a white light source (Agilent 83437A) and light is collected with an Agilent 86140B optical spectrum analyzer.

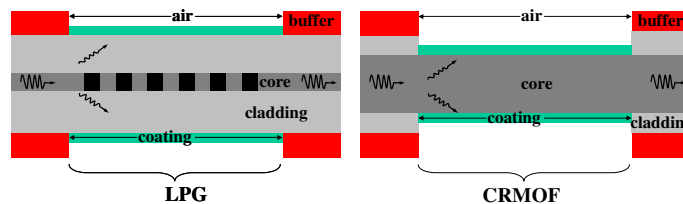


Fig. 1. Optical transmission setup: (a) long period fiber grating; (b) cladding removed multimode optical fiber.

3. Theory

The method used for LPFG simulations is based on the LP mode approximation [4]. This scalar model has been used rather than a vectorial method [7] because the refractive index contrast between the fiber cladding and the coating is low [7]. Consequently, this approximation is valid in this case.

The method used for CRMOF simulations is based on that used in [14]. In order to obtain the transmitted optical power in the structure of Fig. 1 it is important to apply first the attenuated total reflection (ATR) method with a Kretschmann configuration. With this method the reflectivity as a function of wavelength and incidence angle is obtained at the coating - fiber core interface $R(\theta, \lambda)$ [21,22], where λ is the light wavelength and θ the angle of incidence. According to [21], the general expression for calculation of the transmitted optical power is

$$T(\lambda) = \frac{\int_{\theta_c}^{90^\circ} p(\theta) R^{N(\theta)}(\theta, \lambda) d\theta}{\int_{\theta_c}^{90^\circ} p(\theta)} \quad (2)$$

where θ_c is the critical angle, $N(\theta)$ is the number of reflections at the coating - fiber core interface as a function of the angle of incidence, and $p(\theta)$ is the power distribution of the optical source. A broadband source is used in the experiments. However, the light is guided through an optical fiber before it enters the coated region. Consequently, the Gaussian expression is rather preferred [23]:

$$p(\theta) \propto \exp \left[-\frac{\left(\theta - \frac{\pi}{2} \right)^2}{2W^2} \right] \quad (3)$$

It is also important to mention that since the light introduced in the optical fiber is unpolarized, $R^{N(\theta)}(\theta, \lambda)$ can be replaced in expression (2) with the following expression, which considers the reflected light as a combination of the reflected power in TE and TM mode polarization [22]:

$$R^{N(\theta)}(\theta, \lambda) = \frac{R_{TM}^{N(\theta)}(\theta, \lambda) + R_{TE}^{N(\theta)}(\theta, \lambda)}{2} \quad (4)$$

Finally, the wavelength dependence of silica, which is the optical waveguide material, is expressed according to the Sellmeier expression [24], and the wavelength dependence of [PAH + NR/PAA] is modeled with the Lorentz-oscillator model [25]:

$$\varepsilon(E) = \varepsilon(\infty) + \sum_n \frac{A_n}{E_n^2 - E^2 - i\Gamma_n E} \quad (5)$$

where ε is the complex dielectric function, ε_∞ is the high frequency dielectric constant, and A_n , E_n and Γ_n are the amplitude, center energy and broadening of each oscillator. The parameters used are: $n = 1$, $\varepsilon_\infty = 1$, $A_1 = 39.5 \text{ eV}^2$, $E_1 = 5.5 \text{ eV}$ and $\Gamma_1 = 0.19 \text{ eV}$.

4. Results

In this section both simulated and experimental results for both coated LPFG and CRMOF are presented. The two devices are coated with 90 bilayers of [PAH + NR/PAA]. Each bilayer represents a thickness of 14.45 nm.

In Fig. 2 the simulated and experimental results show the evolution of the LPFG resonances as a function of the number of bilayers deposited. The resonances (black regions in the plots) experiment an abrupt wavelength shift between 20 and 40 bilayers. This is caused by a cladding mode reorganization induced by modes guided in the coating.

In Fig. 3, the simulated and experimental results show the evolution of a single resonance (black region in the plot) as a function the number of bilayers deposited on a CRMOF. This resonance is caused by coupling to the coating of the evanescent field of the light guided by the core. The phenomenon is analogous to light propagation through semiconductor coated

waveguides where, for specific thickness values, attenuation maxima of the light propagating through the optical waveguide are obtained [18]. The waveguide, which in our case is the optical fiber core, transports light through a large number of modes. For specific conditions a maximum coupling from these modes to a lossy mode guided in the coating is obtained [15]. Hence, this phenomenon is considered as lossy mode resonance (LMR). Since it occurs when the lossy mode (the mode guided in the coating) is near cut-off, there are mode cut-off thickness values that lead to attenuation maxima [17]. The same phenomenon can be observed if the variable is the wavelength and not the thickness. If the thin-film thickness is fixed, a resonance will be visible in the electromagnetic spectrum for those incident wavelength values where there is a mode near cut-off in the overlay [14]. In Fig. 3, as the coating thickness (proportional to the number of bilayers) increases, an LMR shifts to higher wavelengths. The wavelength range analyzed does not permit to observe the LMR when the first bilayers are deposited. At about 20 bilayers it starts being visible and it leaves the wavelength range analyzed when 40 bilayers are deposited.

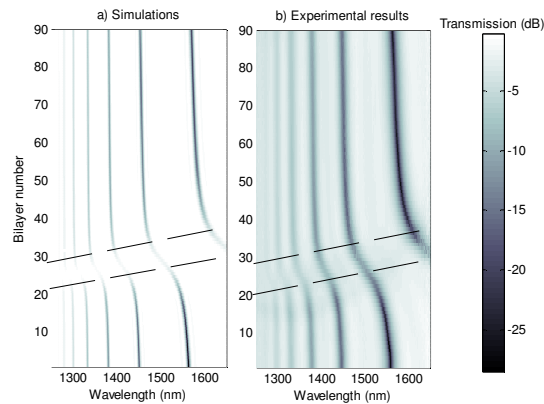


Fig. 2. Response of resonances in an LPFG as a function of coating thickness. The gray scale represents the transmission, with white corresponding to 100% (0dB). Resonances experiment an abrupt wavelength shift between 20 and 40 bilayers (see dotted lines).

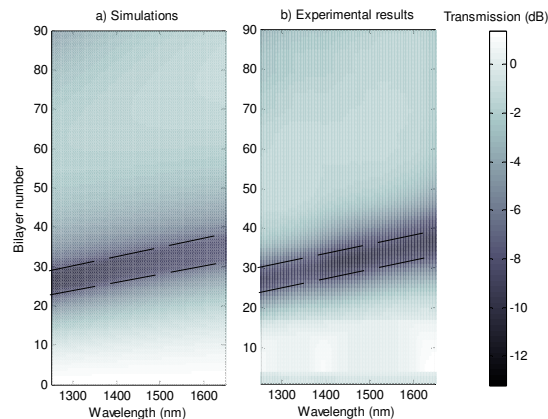


Fig. 3. Response of lossy mode resonances (LMR) in a cladding removed multimode fiber as a function of coating thickness. The gray scale represents the transmission, with white corresponding to 100% (0 dB). The LMR is visible in the spectrum between 20 and 40 bilayers and it is delimited with dotted lines for the sake of comparison with the results of Fig. 2.

In order to understand better the resonances observed in Fig. 2 and 3, a modal analysis is performed. In [7] it is indicated that two modes experiment a transition from being guided in

the core to being guided in the overlay when the coating thickness is increased. This causes a modal redistribution in the LPFG, which occurs at the same bilayer number range. At the same time, there is a reduction in the depth of the LPFG resonances. This effect is appreciated in Fig. 2 (dashed lines). This is caused by change of the coupling condition from the core to the cladding, but also by absorption of energy by lossy modes guided in the coating [7]. In Fig. 4(a) the coupling wavelengths versus coating thickness obtained by applying expression (1) are presented, showing a good similarity with the results of Fig. 2. In Fig. 4(b) the cut-off wavelengths of the lossy modes guided in the coating of the CRMOF are represented as a function of coating thickness. The LMR observed in Fig. 3 is caused by coupling to the two modes whose cut-off wavelengths are represented in Fig. 4(b). In view of the presence of two modes, two LMRs should be expected. However, the central wavelength of each of these two LMRs is so close to each other that it is not possible to distinguish two resonances. Instead, a single resonance is obtained, which is wider than the LPFG resonance bands (see Fig. 5).

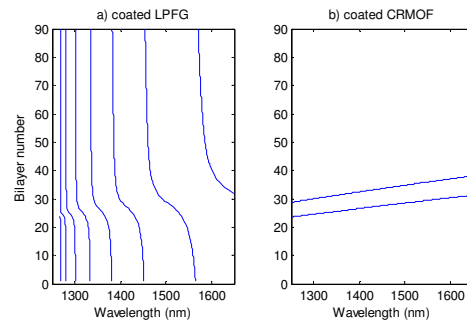


Fig. 4. Modal analysis: (a) Coupling wavelengths as a function of coating thickness for a coated LPFG. (b) cutoff wavelengths for modes in a coated CRMOF.

Both LPFGs and CRMOFs can be used for sensing purposes. However, there are important differences. In a CRMOF, the resonances generated by coating, experiment more abrupt wavelength shifts as a function of thickness than the resonances of LPFGs. The wavelength shift of the first LMR in a CRMOF is rather linear (42.1 nm/bilayer), whereas the wavelength shift in the resonance at 1550 nm in the LPFG is not linear and its maximum is 6.07 nm/bilayer. The positive question for LPFGs is that the full width at half maximum (FWHM) is much narrower than the FWHM of CRMOF based devices. For coatings in and out of the transition region (3 bilayers and 29 bilayers), the FWHM is respectively 25 and 30 nm [Fig. 5(a)]. However, the FWHM for CRMOF devices overcomes the entire spectrum analyzed [Fig. 5(b)]. The conclusion is that the advantage of a more sensitive device becomes a drawback at the time of detecting with accuracy the central wavelength of the resonance. The aim in future works should be to obtain CRMOF based devices with a narrower FWHM, which could be obtained by modifying the core diameter or by using more complex structures.

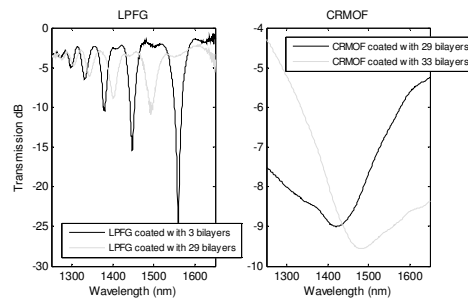


Fig. 5. Transmission spectra for: (a) coated LPFGs (b) coated CRMOFs.

Acknowledgments

The authors acknowledge financial support to the Spanish Ministry of Education and Science-FEDER TEC2009-09210 and TEC2007-67987-C02-02/MIC.